Case Rep Ophthalmol 2011;2:307–313
DOI: 10.1159/000332734
Published online: September 19, 2011

ISSN 1663–2699
www.karger.com/cop

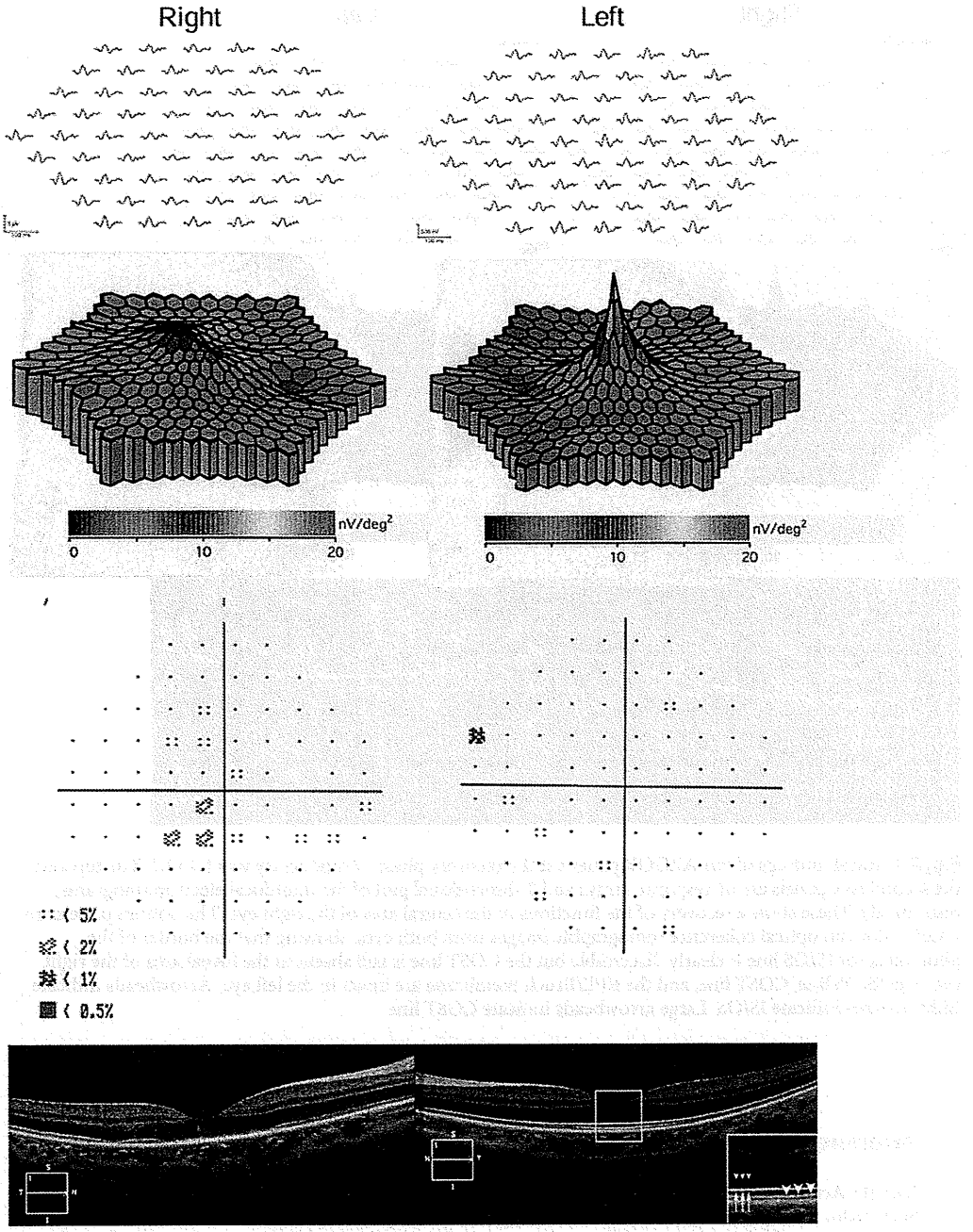

Fig. 1. Clinical findings of a patient at the acute phase of AZOOR. The visual acuity was 0.5 OD and 1.2 OS. First and second rows: mfERGs of the 61 response arrays and 3-dimensional plot of the mfERGs, respectively. These mfERGs show the reduced responses in the area corresponding with the visual field defect. The third row shows the pattern deviation probability map of the Humphrey static visual field tested with central 30-2 program and SITA-Fast strategy (Humphrey Field Analyzer, Carl Zeiss, San Leandro, Calif., USA) for central 30 degree. The mean deviation was –1.04 dB in the right eye and –2.25 dB in the left eye, and the probability map shows a reduced sensitivity in the central area of the right eye. The bottom row shows the Fourier-domain optical coherence tomographic images from the affected right eye and normal left eye. These images show that both the photoreceptor IS/OS line and the COST line between the IS/OS line and RPE are absent in the macula area of the right eye. The IS/OS line, COST line, and the RPE/Bruch membrane are intact in the left eye. Arrowheads indicate ELM. Arrows indicate IS/OS. Large arrowheads indicate COST line.

Case Rep Ophthalmol 2011;2:307–313
DOI: 10.1159/000332734
Published online: September 19, 2011

ISSN 1663–2699
www.karger.com/cop

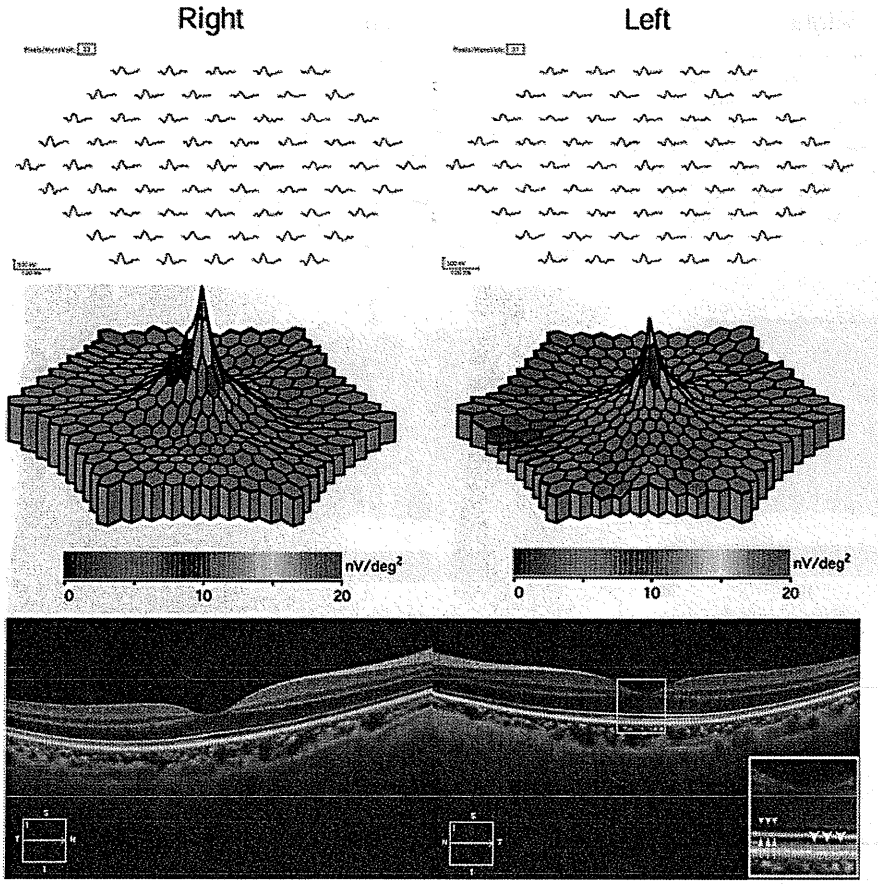

Fig. 2. Clinical findings of our AZOOR patient at the recovery phase. Visual acuity was 1.2 OU. The top and the second row panels are 61 response arrays and 3-dimensional plot of the multifocal electroretinograms, respectively. These show a recovery of the functions in the central area of the right eye. The bottom panels are Fourier-domain optical coherence tomographic images from both eyes, showing that the border of the photoreceptor IS/OS line is clearly discernible but the COST line is still absent in the foveal area of the right eye. The IS/OS line, COST line, and the RPE/Bruch membrane are intact in the left eye. Arrowheads indicate ELM. Arrows indicate IS/OS. Large arrowheads indicate COST line.

References

1 Gass JD: Acute zonal occult outer retinopathy. Donders Lecture: The Netherlands Ophthalmological Society, Maastricht, Holland, June 19, 1992. J Clin Neuroophthalmol 1993;13:79–97.

2 Gass JD, Agarwal A, Scott IU: Acute zonal occult outer retinopathy: a long-term follow-up study. Am J Ophthalmol 2002;134:329–339.

3 Gass JD: Are acute zonal occult outer retinopathy and the white spot syndromes (AZOOR complex) specific autoimmune diseases? Am J Ophthalmol 2003;135:380–381.

4 Spaide RF, Koizumi H, Freund KB: Photoreceptor outer segment abnormalities as a cause of blind spot enlargement in acute zonal occult outer retinopathy-complex diseases. Am J Ophthalmol 2008;146:111–120.

5 Srinivasan VJ, Monson BK, Wojtkowski M, et al: Characterization of outer retinal morphology with high-speed, ultrahigh-resolution optical coherence tomography. Invest Ophthalmol Vis Sci 2008;49:1571–1579.

6 Li D, Kishi S: Loss of photoreceptor outer segment in acute zonal occult outer retinopathy. Arch Ophthalmol 2007;125:1194–1200.

Case Rep Ophthalmol 2011;2:307–313
DOI: 10.1159/000332734
Published online: September 19, 2011

ISSN 1663–2699
www.karger.com/cop

7 Takai Y, Ishiko S, Kagokawa H, Fukui K, Takahashi A, Yoshida A: Morphological study of acute zonal occult outer retinopathy (AZOOR) by multiplanar optical coherence tomography. Acta Ophthalmol 2009;87:408–418.

8 Zibrandtsen N, Munch IC, Klemp K, Jørgensen TM, Sander B, Larsen M: Photoreceptor atrophy in acute zonal occult outer retinopathy. Acta Ophthalmol 2008;86:913–916.

9 Fujiwara T, Imamura Y, Giovinazzo VJ, Spaide RF: Fundus autofluorescence and optical coherence tomographic findings in acute zonal occult outer retinopathy. Retina 2010;30:1206–1216.

10 Ohta K, Sato A, Fukui E: Spectral domain optical coherence tomographic findings at convalescent stage of acute zonal occult outer retinopathy. Clin Ophthalmol 2009;3:423–428.

11 Sugahara M, Shinoda K, Matsumoto CS, Satofuka S, Hanazono G, Imamura Y, Mizota A: Outer retinal microstructure in case of acute idiopathic blind spot enlargement syndrome. Case Rep Ophthalmol 2011;2:116–122.

12 Marmor MF, Fulton AB, Holder GE, Miyake Y, Brigell M, Bach M: Standard for clinical electroretinography (2008 update). Doc Ophthalmol 2009;118:69–77.

13 Byeon SH, Kang SY: Interpretation of outer retina appearance in high-resolution optical coherence tomography. Am J Ophthalmol 2009;147:185–186.

14 Lim JI, Tan O, Fawzi AA, Hopkins JJ, Gil-Flamer JH, Huang D: A pilot study of Fourier-domain optical coherence tomography of retinal dystrophy patients. Am J Ophthalmol 2008;146:417–426.

15 Wakabayashi T, Oshima Y, Fujimoto H, Murakami Y, Sakaguchi H, Kusaka S, Tano Y: Foveal microstructure and visual acuity after retinal detachment repair. Ophthalmology 2009;116:519–528.

16 Wakabayashi T, Fujiwara M, Sakaguchi H, Kusaka S, Oshima Y: Foveal microstructure and visual acuity in surgically closed macular holes: spectral-domain optical coherence tomographic analysis. Ophthalmology 2010;117:1815–1824.

17 Park SJ, Woo SJ, Park KH, Hwang JM, Chung H: Morphologic photoreceptor abnormality in occult macular dystrophy on spectral-domain optical coherence tomography. Invest Ophthalmol Vis Sci 2010;51:3673–3679.

18 Kondo N, Kondo M, Miyake Y: Acute idiopathic blind spot enlargement syndrome: prolonged retinal dysfunction revealed by multifocal electroretinogram technique. Am J Ophthalmol 2001;132:126–128.

19 Hood DC, Zhang X: Multifocal ERG and VEP responses and visual fields: comparing disease-related changes. Doc Ophthalmol 2000;100:115–137.

1040-5488/12/8905-0684/0 VOL. 89, NO. 5, PP. 684–691
OPTOMETRY AND VISION SCIENCE

ORIGINAL ARTICLE

Autosomal Dominant Occult Macular Dystrophy with an *RP1L1* Mutation (R45W)

Takaaki Hayashi*, Tamaki Gekka*, Kenichi Kozaki*, Yasuhiro Ohkuma†, Isako Tanaka*, Hisashi Yamada*, and Hiroshi Tsuneoka*

ABSTRACT

Purpose. To characterize clinical features in occult macular dystrophy (OMD) patients with the *RP1L1* gene mutation (p.R45W), one of two previously described mutations in Japanese OMD patients.

Methods. Mutational screening of the *RP1L1* gene was performed via polymerase chain reaction and direct sequencing for seven unrelated probands (one autosomal dominant and six sporadic probands) with OMD. A comprehensive ophthalmic examination was performed, including Cirrus optical coherence tomography. Full-field electroretinography (ERG), multifocal ERG, and focal macular ERG were performed.

Results. The heterozygous mutation (p.R45W) was found in only one female proband with autosomal dominant OMD, whose mother was also diagnosed with OMD and carried the mutation. Ophthalmoscopy showed bilateral normal fundi in the proband but subtle retinal pigment epithelium mottling in the mother. Both the proband and her mother had typical OMD findings: decreased visual acuity and markedly reduced central responses in the multifocal ERG and focal macular ERG. Although full-field ERG revealed normal rod and standard combined responses, photopic and 30-Hz flicker responses were slightly reduced in both the proband and her mother. Optical coherence tomography revealed that the external limiting membrane and inner segment-outer segment boundary were disorganized despite normal macular thickness in the proband, whereas the mother exhibited macular thinning with discontinuous reflectivity of the external limiting membrane and inner segment-outer segment boundary.

Conclusions. The clinical phenotypes differed between the proband and her mother and were indistinguishable from other sporadic or *RP1L1*-unassociated OMD patients, suggesting that mutation-dependent clinical features may not be present. (Optom Vis Sci 2012;89:684–691)

Key Words: electroretinography, optical coherence tomography, genetics, retinal disorder, macular degeneration, mutation analysis

Occult macular dystrophy (OMD), first described in 1989,[1] is a rare autosomal dominant macular disorder characterized by slowly progressive loss of visual acuity, normal ophthalmoscopic and fluorescein angiographic findings, and normal responses on full-field electroretinography (ERG),[2] but reduced amplitude of focal macular ERG or multifocal ERG.[2,3] In addition to autosomal dominant cases, however, patients with sporadic OMD have also been reported.[3,4] Optical coherence tomography (OCT) findings has revealed outer retinal structural abnormalities at the foveal areas in both autosomal dominant and sporadic OMD patients.[5–8] However, no gene mutation was found in any type of OMD until 2010.

In 2010, a molecular basis of autosomal dominant OMD was first elucidated: two heterozygous missense mutations (p.R45W and p.W960R) in the *RP1L1* gene were identified in four Japanese families, one of which (p.R45W) was found in three of the four families.[9] However, since the discovery of these two *RP1L1* mutations, clinical features of *RP1L1*-associated OMD have not been subsequently described.

Here, we performed mutation analysis of the *RP1L1* gene in Japanese patients with OMD. We identified the clinical features of two patients (a female proband and her mother) in a two-generation family with autosomal dominant OMD who carried the *RP1L1* mutation (p.R45W) heterozygously.

*MD, PhD
†MD
Department of Ophthalmology (TH, TG, KK, YO, HT), Department of Molecular Genetics, Institute of DNA Medicine (HY), The Jikei University School of Medicine, Tokyo, Japan, and Tanaka Eye Clinic, Tokyo, Japan (IT).

METHODS

The study was approved by the institutional review board of The Jikei University School of Medicine. The protocol adhered to the

tenets of the Declaration of Helsinki, and informed consent was obtained from all participants.

Clinical Studies

We investigated the ophthalmic features of two patients in a two-generation Japanese family (JU#0090) with autosomal dominant OMD: a female proband (II-1) and her mother (I-2) (Fig. 1A). Both the proband and her mother underwent a comprehensive ophthalmic examination, including decimal best-corrected visual acuity (BCVA), slitlamp biomicroscopy, dilated ophthalmoscopy, and fluorescein angiography (FA). For retinal scan images, the spectral domain OCT (SD-OCT) (Cirrus HD-OCT; Carl Zeiss Meditec AG, Dublin, CA) was performed using the HD 5 line raster scan protocol and Macular Cube protocol (512 × 128 scan), in which a 6 × 6-mm^2 area of the macula was scanned. Color vision was mono-ocularly evaluated using the Ishihara test (38-plate edition) and the Farnsworth Panel D-15 (Panel D-15). Visual fields were assessed using a Humphrey Field Analyzer (HFA; Carl Zeiss Meditec, Dublin, CA) with the central 30-2 threshold program, and mean deviation (MD) and corrected pattern standard deviation (CPSD) were evaluated. Full-field ERG and multifocal ERG were performed according to the protocols of the International Society for Clinical Electrophysiology of Vision. The procedure and conditions for full-field ERG and multifocal ERG recording have been detailed previously.[10,11] Data analysis of multifocal ERG was performed using the Visual Evoked Response Imaging System (Electro Diagnostic Imaging Inc., San Mateo, CA).

Focal macular ERG findings were recorded using an infrared fundus camera with a stimulus light and background illumination (ER-80; Kowa Company, Tokyo, Japan). The size of the stimulus spot, placed on the macula, was alternated between 5, 10, and 15° in diameter, and the position was confirmed via the infrared fundus monitor. The stimulus and background illumination were generated by white light-emitting diodes with peak spectra of 440 to 460 nm and 540 to 580 nm, respectively. The luminances of the stimulus light and background were 30 and 1.5 cd/m^2. The duration of the stimulation was 100 ms, and responses were amplified and filtered using digital band-pass filters from 5 to 500 Hz (Neuropack μ, MEB-9102; Nihonkoden, Tokyo, Japan). Two to three hundred responses were averaged with a stimulus frequency of 5 Hz.

Molecular Genetic Studies

A total of seven unrelated index probands (one autosomal dominant and six sporadic patients) were clinically diagnosed with OMD at the Jikei University Hospital between April 2001 and March 2007. Genomic DNA was extracted from venous blood samples using a Puregene Blood DNA Isolation kit (Gentra Systems, Minneapolis, MN), and all seven probands underwent molecular analysis. All coding exons (exon 2 to exon 4) of the *RP1L1* gene were amplified via polymerase chain reaction (PCR) using previously reported primers,[12] all of which were produced by Operon Biotechnologies (Tokyo, Japan). The PCR products were purified with a QIAquick PCR Purification kit (Qiagen, Tokyo, Japan) and used as the template for sequencing. Both strands were sequenced on an automated sequencer (3730xl DNA Analyzer; Applied Biosystems, Foster City, CA) using a BigDye Terminator kit V3.1 (Applied Biosystems).

RESULTS

Clinical Findings

The Japanese family (JU#0090) examined in this study included three members with autosomal dominant OMD (Fig. 1A).

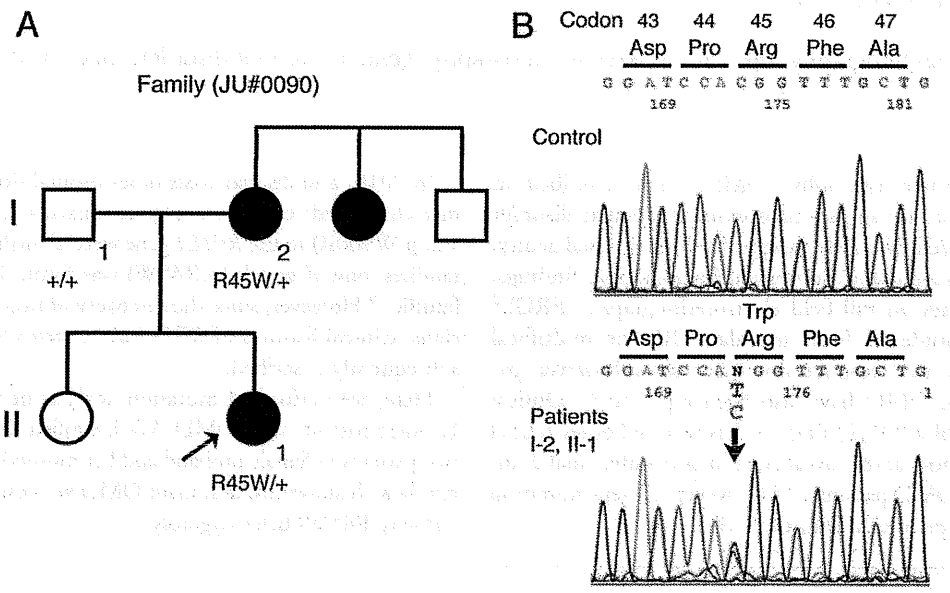

FIGURE 1.

Pedigree of Japanese family JU#0090 and sequence analysis of exon 2 of *RP1L1*. (A) Affected family members are represented by solid circles (females), with an arrow indicating the proband (patient II-1). (B) The arrow indicates the position of the altered nucleotide which resulted in a heterozygously missense mutation (p.R45W) in both patients (I-2 and II-1).

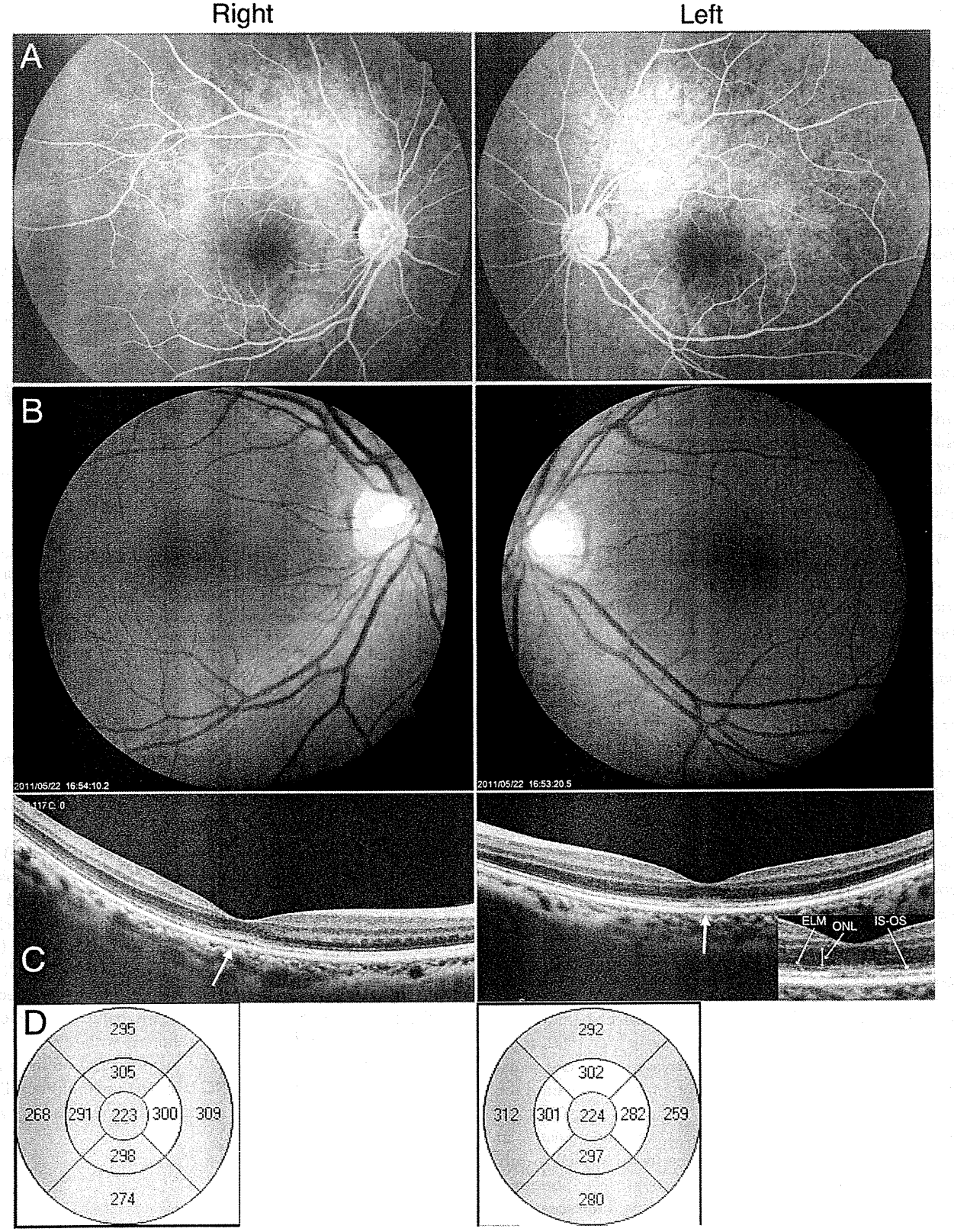

FIGURE 2.

Fluorescein angiograms, fundus photographs, and OCT findings in patient II-1. (A) Late-phase fluorescein angiograms showed unremarkable findings in the maculae but subtle hyperfluorescence along the vascular arcades due to a window defect at the age of 27 years. (B) Fundus photographs showed unremarkable findings at the age of 36 years (C) OCT images of the HD 5 line raster scan showed outer retinal abnormalities only at the foveal areas where the thin reflective band corresponding to the ELM and the hyperreflective band corresponding to the IS/OS boundary are disorganized (arrows); however, the thickness of the ONL was well preserved at the age of 36 years. (D) The macular thickness map of the Macular Cube protocol showed normal macular thickness.

Patient II-1

The proband (patient II-1) was a 27-year-old woman who was referred to the Jikei Hospital in August 2002 complaining of decreased visual acuity. Her BCVA had been 1.0 in both eyes (OU) until the age of 20 years but had deteriorated to 0.7 (sph: −1.75, cyl: −0.25, and axis: 100°) in the right eye (OD) and 0.6 (sph: −2.25, cyl: −0.25, and axis: 130°) in the left eye (OS) at initial evaluation. Anterior segments and media were unremarkable in either eye. Ophthalmoscopy showed no abnormal fundus findings in either eye. Late phase FA showed unremarkable findings in the maculae but subtle hyperfluorescence along the vascular arcades due to a window defect in OU (Fig. 2A).

The patient identified 6/25 (OD) and 4/25 (OS) plates in the Ishihara test, and the Farnsworth Panel D-15 showed no errors in either eye. The HFA pattern deviation plots showed no significant defects, with MD values of −1.77 (OS) and −2.18 (OD) dB, and the CPSD values were 1.85 (OS) and 0.59 (OD) dB (Fig. 3A). The full-field ERG demonstrated normal rod responses in the OD (reliable data were not obtained from the OS) and normal standard combined responses, and photopic and 30-Hz flicker responses were slightly reduced in OU (Fig. 4A).

Nine years later after initial presentation (at the age of 36 years), the patient's BCVA had decreased to 0.4 in OU. Although ophthalmoscopy showed unremarkable findings in OU (Fig. 2B), SD-OCT images of the HD 5 line raster scan revealed outer retinal abnormalities at the foveal areas where the thin reflective band corresponding to the external limiting membrane (ELM) and the hyperreflective band corresponding to the inner segment-outer segment (IS/OS) boundary were disorganized; however, the thickness of the outer nuclear layer (ONL) remained well preserved in OU (Fig. 2C).

The macular thickness map of the Macular Cube protocol showed normal macular thickness (Fig. 2D). The focal macular ERG demonstrated non-detectable responses at 5°, severely reduced responses at 10°, and reduced responses at 15° in OU (Fig. 4B). In multifocal ERG, the central (ring 1) responses were absent, paracentral (ring 2) responses were greatly reduced, and the outer waveforms (rings 3 to 5) were about one-third of the normal responses in OU (Fig. 4C).

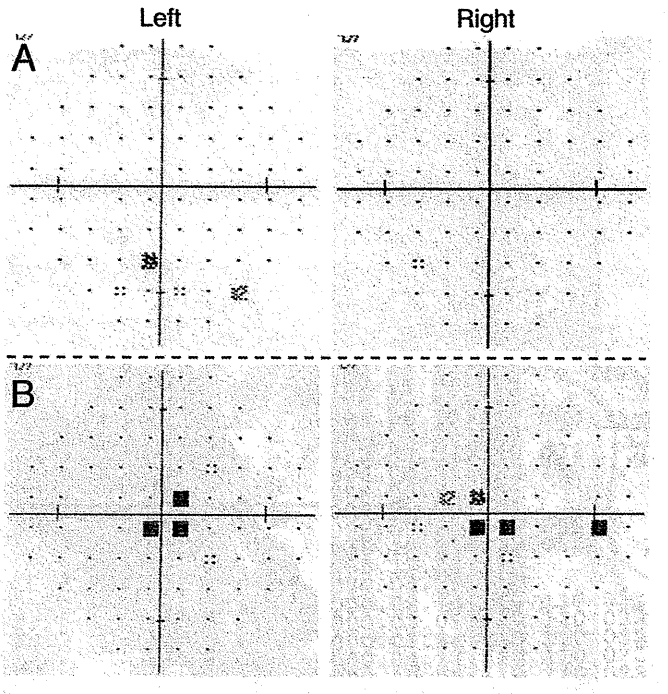

FIGURE 3.

Visual fields using the HFA with the central 30-2 threshold program. (A) No significant visual field defects were detected. MD was −1.77 (left eye) and −2.18 dB (right eye), and CPSD was 1.85 (left eye) and 0.59 dB (right eye) in patient II-1 at the age of 27 years. (B) Central visual field defects were detected. MD was +1.95 (left eye) and +1.74 dB (right eye), and CPSD was 2.81 dB ($p < 10\%$) (left eye) and 2.56 dB ($p < 10\%$) (right eye) in patient I-2 at the age of 56 years.

Patient I-2

The proband's affected mother (patient I-2) first underwent ophthalmic examination at Tanaka Eye Clinic in June 1992, at the age of 49 years, after experiencing a decrease in bilateral visual acuity. Although she had had a BCVA of 1.0 bilaterally until the age of 30 years, her BCVA at initial evaluation was 0.6 (sph: +0.50), and anterior segments and media were unremarkable in OU. She was subsequently referred to the Jikei Hospital in July 1992 for further examination. Ophthalmoscopy showed abnormal macular ring reflex, and FA revealed small, hyperfluorescent dots due to retinal pigment epithelium alterations in both maculae (Fig. 5A).

Goldmann perimetry conducted at the age of 51 years demonstrated bilateral central scotomas (I-1 targets) within 5 to 7° of point of fixation. The Farnsworth Panel D-15 was arranged in a deutan pattern in each eye. By the age of 56 years, her BCVA had decreased to 0.4 in OU, and HFA pattern deviation plots showed central visual field defects: MD values were +1.95 (OS) and +1.74 (OD) dB, and CPSD values were 2.81 ($p < 10\%$) (OS) and 2.56 ($p < 10\%$) (OD) dB (Fig. 3B).

At the age of 70 years, her BCVA had decreased to 0.3 (OD) and 0.2 (OS). Ophthalmoscopy showed subtle retinal pigment epithelium mottling in OU (Fig. 5B). The SD-OCT of the HD 5 line raster scan showed thinning of the ONL and discontinuous reflectivity of the ELM and IS/OS lines at the foveal areas in OU (Fig. 5C). In addition, a hyporeflective zone (described elsewhere[13]) was noted (Fig. 5C) between the IS/OS line and the hyperreflective retinal pigment epithelium/choriocapillaris band. The macular thickness map showed significant thinning within the 1- and 3-mm rings and normal thickness of the outer (3 to 6 mm) ring (Fig. 5D) bilaterally. Full-field ERG (Fig. 4A) and multifocal ERG (Fig. 4C) examinations revealed the same abnormal findings as in patient II-1.

Molecular Genetic Findings

Mutation analysis of the *RP1L1* gene revealed that only patient II-1 in JU#0090 (one of the seven unrelated probands) had a heterozygous variant (c.133C>T in exon 2). This variant results in the substitution of tryptophan (TGG) for arginine (CGG) at amino acid position 45 (Fig. 1B). This missense mutation (p.R45W) was one of the two mutations previously reported in the

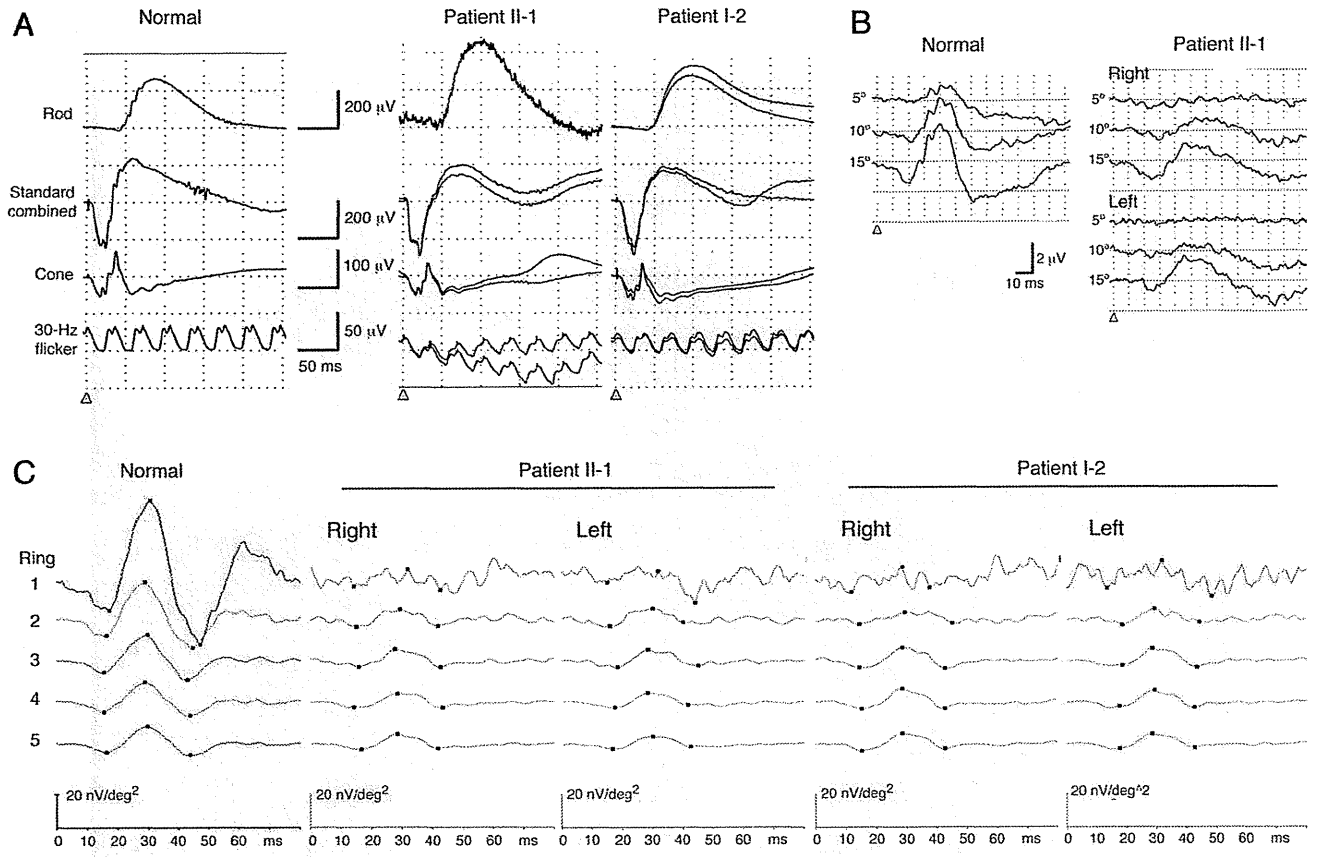

FIGURE 4.

Full-field ERG, focal macular ERG, and multifocal ERG. (A) Full-field ERG showed normal rod responses, normal standard combined responses, and slightly reduced photopic and 30-Hz flicker responses in patient II-1 at the age of 27 years and patient I-2 at the age of 70 years. (B) Focal macular ERG showed non-detectable responses at 5° spots, severely reduced responses at 10° spots, and reduced responses at 15° spots in patient II-1 at the age of 36 years. (C) Multifocal ERG showed absence of central (ring 1) responses, greatly reduced paracentral (ring 2) responses, and about one-third of normal responses in outer waveforms (rings 3 to 5) in patient II-1 at the age of 36 years and patient I-2 at the age of 70 years.

RP1L1 gene.[9] No other pathological variation of this gene was detected.

Although blood samples were available from the parents (I-1 and I-2) of patient II-1, none were obtained from the patient's mother's sister, who was also diagnosed with OMD. Like patient II-1, the affected mother (patient I-2) also carried a heterozygous mutation in the *RP1L1* gene, although the asymptomatic father (I-1) did not.

This mutation was not found in any of 100 Japanese individuals without any retinal diseases or in the Japanese single nucleotide polymorphisms database (http://snp.ims.u-tokyo.ac.jp).

DISCUSSION

At present, no studies have reported on the clinical features of OMD associated with *RP1L1* mutations since the discovery of those same mutations (p.R45W and p.W960R) in four Japanese families with autosomal dominant OMD.[9] In this study, both patients with the p.R45W mutation had ocular findings typical of OMD, markedly reduced central responses on either or both focal macular ERG (Fig. 4B) and multifocal ERG (Fig. 4C), and foveal structural abnormalities in the SD-OCT (Figs. 2C, 5C). However, ophthalmoscopic findings revealed subtle retinal pigment epithelium mottling (Fig. 5B) confirmed as small hyperfluorescent dots on FA in patient I-2 (Fig. 5A), although no similar abnormality was seen in patient II-1 (Fig. 2B). In addition to the ophthalmoscopic abnormalities in patient I-2, we observed slightly reduced photopic/30-Hz flicker responses (Fig. 4A) in both patients, findings which were unusual and differed from those previously reported,[1–3] as the diagnostic definition of OMD requires a normal ophthalmoscopic appearance and normal photopic/30-Hz flicker responses on full-field ERG. However, bull's eye maculopathy has been observed in only one patient of an autosomal dominant OMD family.[2]

Regarding OCT findings, a previous study first reported that mean foveal thickness in 11 patients with OMD was significantly thinner than in 20 age-matched controls[5]—a finding confirmed by subsequent reports[6,8,14]—demonstrating that foveal thickness determined using SD-OCT was thinned in all OMD patients. Foveal structural abnormalities observed using SD-OCT were recently reported in seven patients with autosomal dominant OMD, with IS/OS line irregularity at the foveal area noted in all seven, although *RP1L1* mutational analysis was not performed.[7] This previous observation of IS/OS line irregularity[7] was similar to the disorganized ELM and IS/OS lines noted in patient II-1 (Fig. 2C).

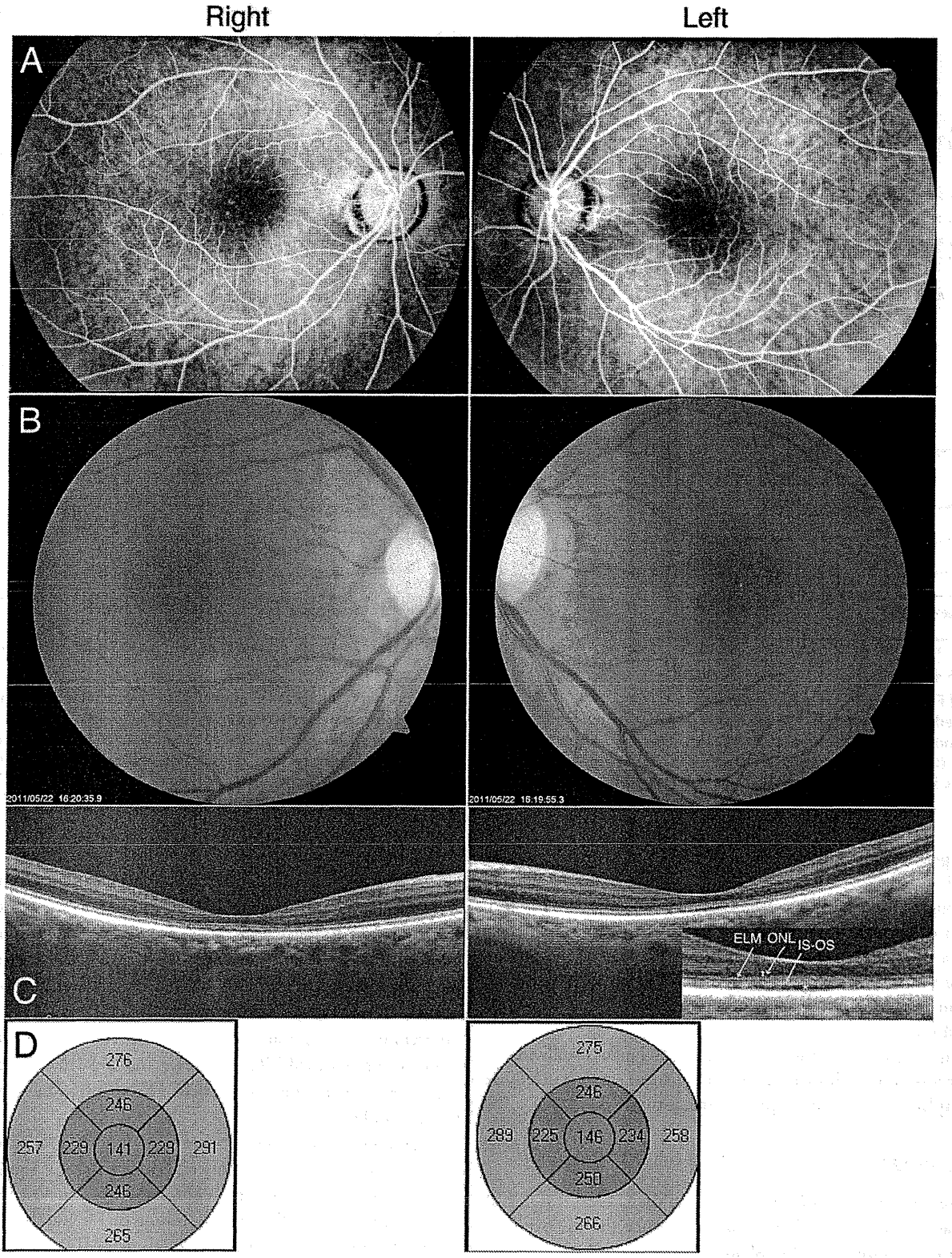

FIGURE 5.

Fluorescein angiograms, fundus photographs, and OCT findings in patient I-2. (A) Middle-phase fluorescein angiograms showed small hyperfluorescent dots due to retinal pigment epithelium alterations in the maculae at the age of 49 years. (B) Fundus photographs showed subtle retinal pigment epithelium mottling at the age of 70 years. (C) OCT images of the HD 5 line raster scan showed thinning of the ONL and discontinuous reflectivity of the ELM and IS/OS boundary at the foveal areas, and a hyporeflective zone (asterisk) can be seen between the IS/OS line and the hyperreflective retinal pigment epithelium/choriocapillaris band at the age of 70 years. (D) The macular thickness map of the Macular Cube protocol showed significant thinning within the 1- and 3-mm rings (red color) and normal thickness of the outer (3 to 6 mm) ring (green color).

In addition, macular thickness mapping revealed normal macular thickness (even in the central 1-mm ring) in patient II-1 (Fig. 2D) and significant thinning of the 1- and 3-mm rings associated with thinning of the ONL in patient I-2 (Fig. 5D). The normal macular thickness in patient II-1, who had relatively good visual fields (Fig. 3A), may be explained by the previous finding that some OMD patients do exhibit normal foveal thickness.[5,6]

A hyporeflective zone with either completely disrupted or discontinuous IS/OS junction reflectivity has been described in patients with achromatopsia[13] who have no functional cone photoreceptor cells. In this study, patient I-2 possessed such a hyporeflective zone with discontinuous reflectivity of the IS/OS lines at the foveal area (Fig. 5C), a phenomenon which has also been observed in other previously reported OMD patients.[8] Because cone photoreceptor density is maximal at the foveal region,[15,16] the hyporeflective zone present in patient I-2 resulted in a decreased number of cone photoreceptor cells, explaining the patient's color-vision and central visual-field defects (Fig. 3B), decreased visual acuity, and reduced multifocal ERG responses (Fig. 4C).

However, it should be noted that the above-mentioned SD-OCT findings differed between patients II-1 and I-2 with regard to foveal structure and ONL thickness. Differences in foveal structural abnormalities even between members of the same family may be due to differing levels of severity, differing disease stages, or phenotypic variability. Given that either preserved or thinned ONL thickness is relevant to disease progression, we hypothesize that foveal microstructural changes in the ELM and IS/OS lines with preserved foveal thickness are evident in early stages of the disease, as with patient II-1, whereas discontinuous reflectivity or disruption of the IS/OS lines with thinned foveal thickness are more typically observed in advanced stages, as with patient I-2. An SD-OCT study demonstrated that visual acuity was proportional to central foveal thickness in eight OMD patients,[6] supporting this hypothesis.

Despite the fact that the RP1L1 transcript and protein are expressed in both rod and cone photoreceptor cells,[12,17] all electroretinographic, visual-field, and SD-OCT abnormalities in these patients appear to be confined to the central retina. A recent study has suggested that both *RP1* and *RP1L1*, the genes of which share 63% identity at the amino acid level,[12,18] play essential and synergistic roles in photosensitivity and outer segment morphogenesis in photoreceptor cells.[19] *RP1* missense mutations and truncated mutations may be involved in the pathogenesis of autosomal dominant retinitis pigmentosa through a dominant negative effect.[20,21] Taken together, these findings suggest that the *RP1L1* mutation (p.R45W) may play a role in OMD etiology through a similar mechanism to *RP1* mutations, subsequently affecting the central retina with its maximum cone photoreceptor density.

In conclusion, this is the first report that described clinical characteristics of autosomal dominant OMD with the heterozygous mutation (p.R45W) in the *RP1L1* gene. Indeed, ophthalmoscopic macular changes and subtle reductions in photopic/30 Hz flicker responses can be seen in OMD patients with the mutation. SD-OCT findings differed between our patients and were indistinguishable from those obtained in other sporadic or *RP1L1*-unassociated OMD patients in whom other genetic loci may be involved. Further study will be required to determine whether *RP1L1* mutation-dependent clinical features are present.

ACKNOWLEDGMENTS

This work was supported by grants from the Ministry of Education, Culture, Sports, Science and Technology of Japan (Grant-in-Aid for Scientific Research; to TH); the Ministry of Health, Labor and Welfare of Japan (to TH); The Jikei University Research Fund (to TH); and the Vehicle Racing Commemorative Foundation (to TH and HT).

Received September 27, 2011; accepted November 4, 2011.

REFERENCES

1. Miyake Y, Ichikawa K, Shiose Y, Kawase Y. Hereditary macular dystrophy without visible fundus abnormality. Am J Ophthalmol 1989; 108:292–9.
2. Miyake Y, Horiguchi M, Tomita N, Kondo M, Tanikawa A, Takahashi H, Suzuki S, Terasaki H. Occult macular dystrophy. Am J Ophthalmol 1996;122:644–53.
3. Piao CH, Kondo M, Tanikawa A, Terasaki H, Miyake Y. Multifocal electroretinogram in occult macular dystrophy. Invest Ophthalmol Vis Sci 2000;41:513–7.
4. Lyons JS. Non-familial occult macular dystrophy. Doc Ophthalmol 2005;111:49–56.
5. Kondo M, Ito Y, Ueno S, Piao CH, Terasaki H, Miyake Y. Foveal thickness in occult macular dystrophy. Am J Ophthalmol 2003;135: 725–8.
6. Brockhurst RJ, Sandberg MA. Optical coherence tomography findings in occult macular dystrophy. Am J Ophthalmol 2007;143: 516–8.
7. Fujinami K, Tsunoda K, Hanazono G, Shinoda K, Ohde H, Miyake Y. Fundus autofluorescence in autosomal dominant occult macular dystrophy. Arch Ophthalmol 2011;129:597–602.
8. Kim YG, Baek SH, Moon SW, Lee HK, Kim US. Analysis of spectral domain optical coherence tomography findings in occult macular dystrophy. Acta Ophthalmol 2011;89:52–6.
9. Akahori M, Tsunoda K, Miyake Y, Fukuda Y, Ishiura H, Tsuji S, Usui T, Hatase T, Nakamura M, Ohde H, Itabashi T, Okamoto H, Takada Y, Iwata T. Dominant mutations in *RP1L1* are responsible for occult macular dystrophy. Am J Hum Genet 2010;87:424–9.
10. Hayashi T, Gekka T, Takeuchi T, Goto-Omoto S, Kitahara K. A novel homozygous *GRK1* mutation (P391H) in 2 siblings with Oguchi disease with markedly reduced cone responses. Ophthalmology 2007;114:134–41.
11. Takeuchi T, Hayashi T, Bedell M, Zhang K, Yamada H, Tsuneoka H. A novel haplotype with the R345W mutation in the *EFEMP1* gene associated with autosomal dominant drusen in a Japanese family. Invest Ophthalmol Vis Sci 2010;51:1643–50.
12. Bowne SJ, Daiger SP, Malone KA, Heckenlively JR, Kennan A, Humphries P, Hughbanks-Wheaton D, Birch DG, Liu Q, Pierce EA, Zuo J, Huang Q, Donovan DD, Sullivan LS. Characterization of *RP1L1*, a highly polymorphic paralog of the retinitis pigmentosa 1 (*RP1*) gene. Mol Vis 2003;9:129–37.
13. Thomas MG, Kumar A, Kohl S, Proudlock FA, Gottlob I. High-resolution in vivo imaging in achromatopsia. Ophthalmology 2011; 118:882–7.
14. Koizumi H, Maguire JI, Spaide RF. Spectral domain optical coherence tomographic findings of occult macular dystrophy. Ophthalmic Surg Lasers Imaging 2009;40:174–6.
15. Curcio CA, Sloan KR, Jr., Packer O, Hendrickson AE, Kalina RE. Distribution of cones in human and monkey retina: individual variability and radial asymmetry. Science 1987;236:579–82.

16. Chui TY, Song H, Burns SA. Adaptive-optics imaging of human cone photoreceptor distribution. J Opt Soc Am (A) 2008;25: 3021–9.
17. Conte I, Lestingi M, den Hollander A, Alfano G, Ziviello C, Pugliese M, Circolo D, Caccioppoli C, Ciccodicola A, Banfi S. Identification and characterisation of the retinitis pigmentosa 1-like1 gene (RP1L1): a novel candidate for retinal degenerations. Eur J Hum Genet 2003;11:155–62.
18. Blanton SH, Heckenlively JR, Cottingham AW, Friedman J, Sadler LA, Wagner M, Friedman LH, Daiger SP. Linkage mapping of autosomal dominant retinitis pigmentosa (RP1) to the pericentric region of human chromosome 8. Genomics 1991;11:857–69.
19. Yamashita T, Liu J, Gao J, LeNoue S, Wang C, Kaminoh J, Bowne SJ, Sullivan LS, Daiger SP, Zhang K, Fitzgerald ME, Kefalov VJ, Zuo J. Essential and synergistic roles of RP1 and RP1L1 in rod photoreceptor axoneme and retinitis pigmentosa. J Neurosci 2009;29: 9748–60.
20. Chiang SW, Wang DY, Chan WM, Tam PO, Chong KK, Lam DS, Pang CP. A novel missense RP1 mutation in retinitis pigmentosa. Eye (Lond) 2006;20:602–5.
21. Zhang X, Chen LJ, Law JP, Lai TY, Chiang SW, Tam PO, Chu KY, Wang N, Zhang M, Pang CP. Differential pattern of RP1 mutations in retinitis pigmentosa. Mol Vis 2010;16:1353–60.

Takaaki Hayashi
Department of Ophthalmology
The Jikei University School of Medicine
3-25-8 Nishi-shimbashi
Minato-ku, Tokyo 105-8461
Japan
e-mail: taka@jikei.ac.jp

Short Communication

Ophthalmic Research

Ophthalmic Res 2011;46:175–180
DOI: 10.1159/000325024

Received. October 22, 2010
Accepted after revision: February 3, 2011
Published online. March 29, 2011

Macular Dysfunction in Oguchi Disease with the Frequent Mutation 1147delA in the *SAG* Gene

Takaaki Hayashi[a] Satoshi Tsuzuranuki[a] Kenichi Kozaki[a] Mitsuyoshi Urashima[b] Hiroshi Tsuneoka[a]

[a]Department of Ophthalmology and [b]Division of Molecular Epidemiology, The Jikei University School of Medicine, Tokyo, Japan

Key Words
Full-field electroretinography · Multifocal electroretinography · Mutation · Optical coherence tomography · *SAG* gene

Abstract
Aim/Background: A 1-bp deletion (1147delA) in the *SAG* (also known as arrestin or S-antigen) gene is the most frequently seen mutation in Japanese patients suffering from Oguchi disease, a recessively inherited stationary night blindness. We investigated macular function in a patient with Oguchi disease with the 1147delA mutation. ***Methods:*** A 43-year-old Japanese male patient was diagnosed with Oguchi disease. The patient underwent complete ophthalmic examinations, including spectral-domain optical coherence tomography and Humphrey visual field testing. Full-field electroretinograms (ff-ERG) and multifocal ERG (mf-ERG) were recorded. Mutational analysis of the *SAG* gene was performed. ***Results:*** Corrected visual acuity was good in both eyes. Funduscopy showed retinal pigment epithelium atrophy along the vascular arcade bilaterally. The inner segment-outer segment (ISOS) boundary lines were preserved in the foveal and parafoveal areas, whereas ISOS boundary defects and thinning of the outer nuclear layer (ONL) were seen outside the preserved ISOS boundary. Humphrey testing showed significant paracentral field defects in both eyes. In addition to an absence of rod responses, cone and 30-Hz flicker responses were markedly reduced in ff-ERG. The central (ring 1) and paracentral (ring 2) responses with normal latencies were relatively preserved, but the outer waveforms (rings 3–5) were attenuated and prolonged in mf-ERG. The deletion mutation (1147delA) was identified homozygously. ***Conclusions:*** The reduced/delayed mf-ERG responses and visual field defects in paracentral macula areas are most likely to be correlated with ISOS boundary defects and thinning of the ONL. Macular dysfunction can occur in Oguchi disease with the 1147delA mutation in the *SAG* gene.

Introduction

Oguchi disease, first described in 1907 [1], is a rare autosomal-recessive form of congenital stationary night blindness, a non-progressive retinal disorder in which all other visual functions – including visual acuity, visual field, and color vision – are usually normal. One feature

KARGER

Fax +41 61 306 12 34
E-Mail karger@karger.ch
www.karger.com

0030–3747/11/0464–0175$38.00/0

Accessible online at:
www.karger.com/ore

Takaaki Hayashi, MD, PhD
Department of Ophthalmology, The Jikei University School of Medicine
3-25-8 Nishi-shimbashi, Minato-ku
Tokyo 105-8461 (Japan)
Tel. +81 3 3433 1111, ext. 3581, E-Mail taka@jikei.ac.jp

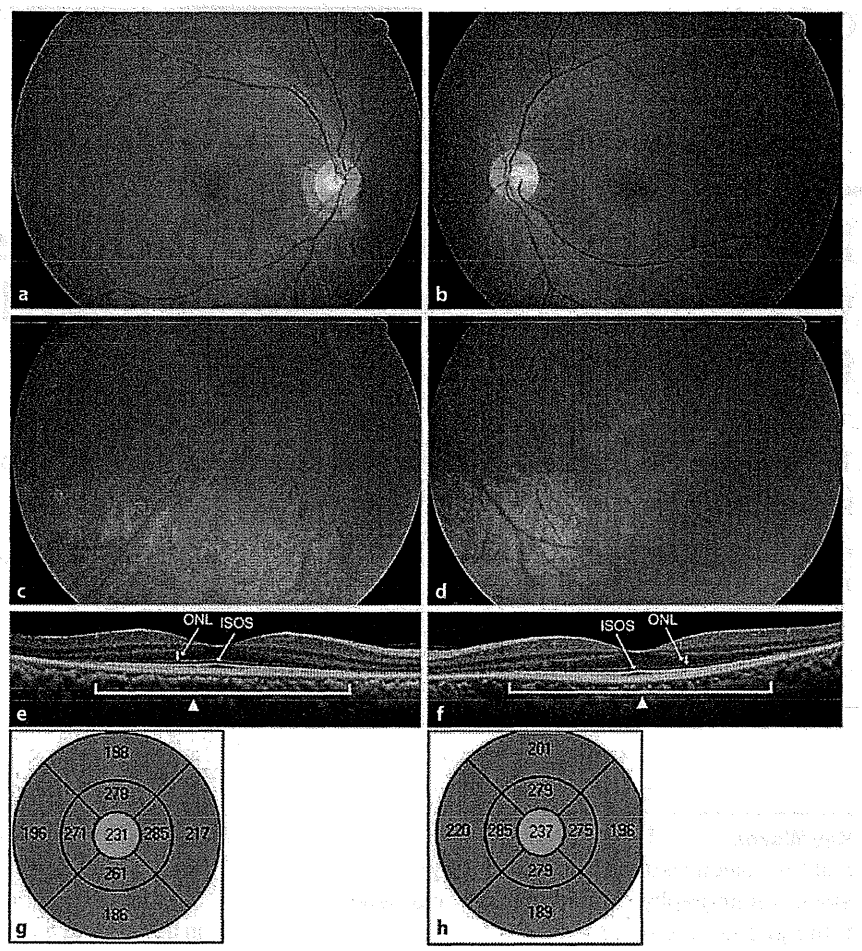

Fig. 1. Fundus photographs (**a–d**) and OCT findings (**e–h**). Retinal pigment epithelium atrophy is seen along the vascular arcade in OD (**a**) and OS (**b**). Golden-yellow discoloration is seen in the inferior mid-periphery in OD (**c**) and OS (**d**). ISOS boundary lines are preserved in the foveal and parafoveal areas (arrowheads), whereas ISOS boundary defects and thinning of the ONL are seen outside the preserved ISOS boundary in OD (**e**) and OS (**f**). The maps of macular thickness show preserved foveal thickness (green), but marked retinal thinning of the perifoveal region (red) in OD (**g**) and OS (**h**).

of the disease is a golden-yellow discoloration of the fundus that disappears in the long dark-adapted state (Mizuo-Nakamura phenomenon) [2]. Full-field electroretinograms (ff-ERG) show the absence of rod b-waves after 30 min of dark adaptation, and reduced a-waves and extremely reduced b-waves (negative type) in standard combined responses [3, 4]. In contrast, the single-flash cone and 30-Hz flicker responses are within normal limits [3, 4].

In 1995, a homozygous 1-bp deletion (1147delA, counted from the 5′ end of the previously published S-antigen cDNA sequence [5]) mutation in the *SAG* (also known as arrestin or S-antigen) gene was identified in 5 out of 6 unrelated Japanese patients with Oguchi disease [6]. Subsequently, 3 mutations [deletion of exon 5, Val380Asp, and Ser536 (4-bp del)] in the *GRK1* (rhodopsin kinase) gene were also reported in European patients with Oguchi disease [7]. The *SAG* mutation (1147delA), also called c.924delA (counted from the translation initiation site), has been most frequently seen in Japanese patients identified to date [8–12]. Saga et al. [11] demonstrated that a total of 9 Oguchi disease patients with the 1147delA mutation had the same haplotype at codon 403 and IVS6-18, suggesting that the 1147delA mutation may be inherited from a single founder. Although previous studies have shown the presence of reduced cone responses in some Oguchi disease patients with the frequent 1147delA mutation [8, 9], no studies have focused on the relationships between macular function and morphology.

This report was conducted to investigate macular function electroretinographically and anatomical features of the macula using optical coherence tomography (OCT) in an Oguchi disease patient with the frequent 1147delA mutation in the *SAG* gene.

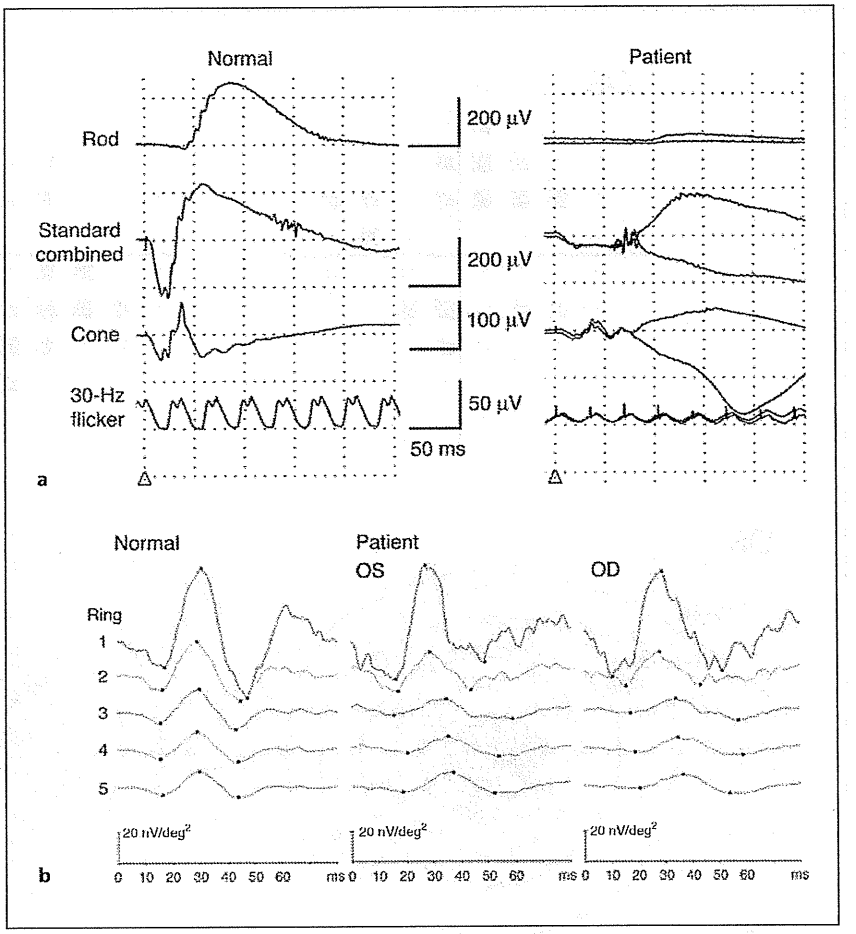

Fig. 2. ff-ERG (**a**) and mf-ERG (**b**). In the patient, ff-ERG (**a**) showed no rod responses, and an extreme reduction in a-wave amplitudes with almost extinguished b-wave amplitudes in standard combined ERG. Cone ERG revealed reduced responses in both a- and b-waves (approximately 25% of normal). Responses in 30-Hz flicker ERG showed reduced amplitudes (approximately 30% of normal). Ring averages (rings 1–5) of mf-ERG (**b**) are depicted. In the patient, the central (ring 1) and paracentral (ring 2) responses with normal latencies were relatively preserved, but the outer waveforms (rings 3–5) were attenuated and prolonged in both eyes.

Case Report

A 43-year-old Japanese male patient, who presented with a history of night blindness since childhood, was referred to our hospital. On the initial evaluation, his decimal best corrected visual acuity was 1.0 (sph –0.50, cyl –1.00, axis 35°) in oculus dexter (OD) and 1.5 (sph –0.25, cyl –0.75, axis 120°) in oculus sinister (OS). Anterior segments and media were unremarkable, except mild corneal opacity in both eyes. Funduscopy showed the retinal pigment epithelium atrophy along the vascular arcade (fig. 1a, b) and golden-yellow discoloration in the mid-periphery (fig. 1c, d), but there were neither retinal bone spicule pigmentation nor attenuation of the peripheral retinal vessels in both eyes. OCT (Cirrus HD-OCT, Carl Zeiss Meditec AG, Dublin, Calif., USA) showed that the inner segment-outer segment (ISOS) boundary lines were preserved in the foveal and parafoveal areas, consistent with the finding that best corrected visual acuity was normal; however, ISOS boundary defects and thinning of the outer nuclear layer (ONL) were seen outside the preserved ISOS boundary (fig. 1e, f). The maps of macular thickness demonstrated preserved foveal thickness, but marked retinal thinning of the perifoveal region in both eyes (fig. 1g, h).

The ff-ERG and multifocal ERG (mf-ERG) were recorded according to the International Society for Clinical Electrophysiology of Vision protocol, and the procedure and conditions have been reported previously [13, 14]. In the ff-ERG (fig. 2a), no rod responses were detected. Standard combined ERG showed an extreme reduction in a-wave amplitudes with almost extinguished b-wave amplitudes. Cone ERG results revealed reduced responses in both a- and b-waves (approximately 25% of normal in both eyes). Responses in 30-Hz flicker ERG showed reduced amplitudes (approximately 30% of normal in both eyes). Implicit times of all ff-ERG responses were normal. Ring averages (rings 1–5) of mf-ERG, recorded with a stimulus size of 61 hexagons, were measured. The central (ring 1) and paracentral (ring 2) responses with normal latencies were relatively preserved, but the outer waveforms (rings 3–5) were attenuated and prolonged in both eyes (fig. 2b).

For visual field assessment, the Humphrey Field Analyzer II (Carl Zeiss Meditec AG) was used to perform the central 30-2

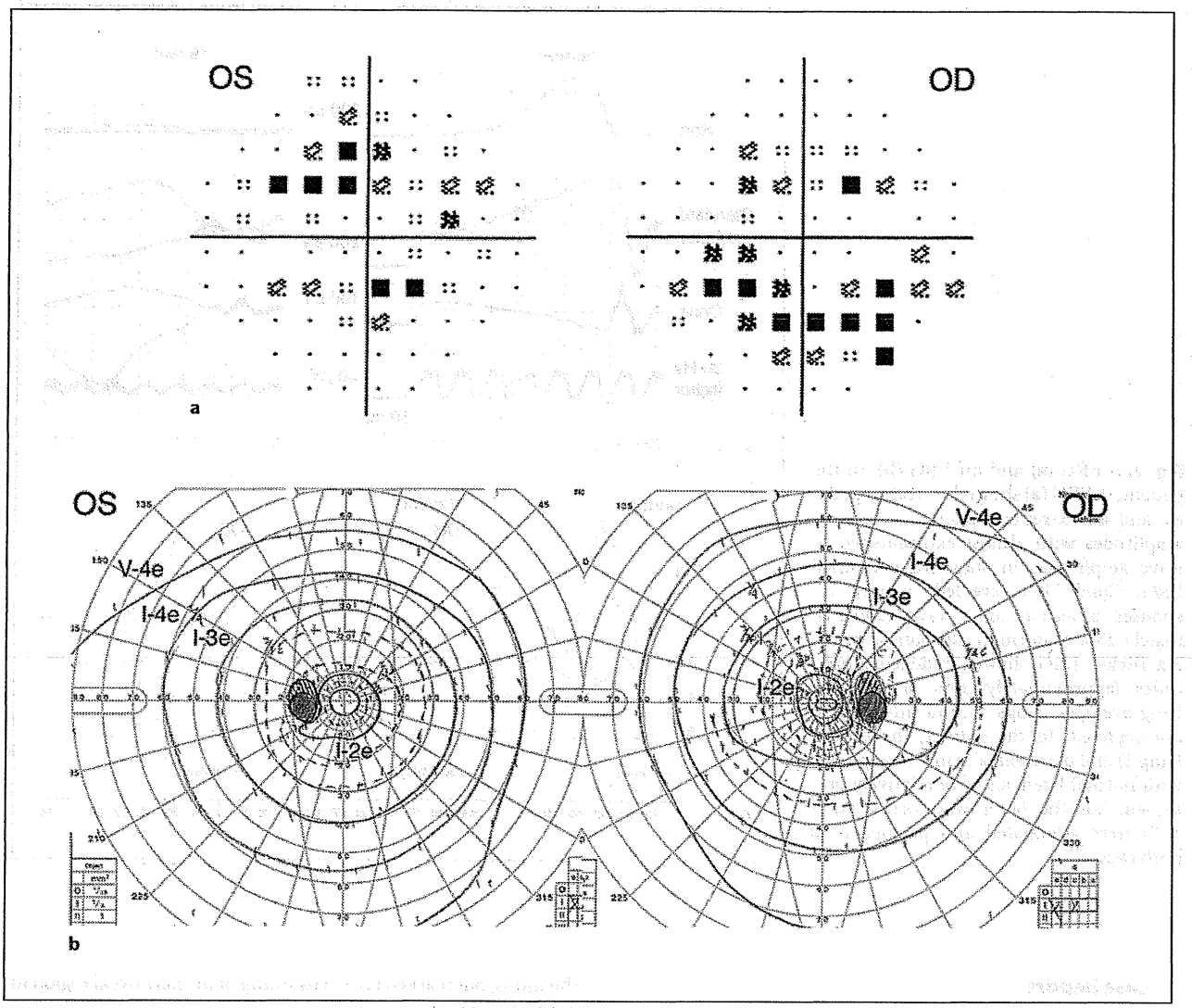

Fig. 3. The pattern deviation plots using the Humphrey Field Analyzer II (**a**) show significant paracentral field defects in both eyes. Goldmann perimetry (**b**) shows no constriction of peripheral isopters (V-4e and I-4e), although the visual fields of the central isopter (I-2e) are moderately constricted in both eyes.

Swedish Interactive Threshold Algorithm standard program, showing significant paracentral field defects in the pattern deviation plots in both eyes (fig. 3a): the mean deviation was –3.55 dB ($p < 2\%$) in OS and –7.71 dB ($p < 0.5\%$) in OD; and the pattern standard deviation was 3.48 dB ($p < 2\%$) in OS and 3.69 dB ($p < 2\%$) in OD. On the other hand, Goldmann perimetry showed no constriction of peripheral isopters (V-4e and I-4e), although the visual fields of central isopter (I-2e) were moderately constricted in both eyes (fig. 3b), compatible with the Humphrey Field Analyzer findings.

For molecular genetic analysis, the research protocol was approved by the institutional review board of The Jikei University School of Medicine. The protocol adhered to the tenets of the Declaration of Helsinki, and informed consent was obtained from all participants. Coding regions of the *SAG* and the *GRK1* genes, containing exon/intron boundaries, were analyzed using polymerase chain reaction followed by sequencing as previously described [14]. A homozygous deletion mutation (1147delA or c.924delA) in exon 11 of the *SAG* gene was identified. No *GRK1* mutation was found in the patient. The patient's parents, who carry the 1147delA mutation heterozygously, had no ocular symptoms.

Discussion

Molecular genetic analysis identified a homozygous deletion mutation (1147delA) in the *SAG* gene, which is the most frequently seen mutation in Japanese patients with Oguchi disease identified to date [6, 8–12], although other *SAG* mutations (Arg175stop and Arg292stop) have also been identified [15]. Nakazawa et al. [8] reported 8 Oguchi disease patients with the 1147delA mutation, 3 of whom had slightly reduced 30-Hz flicker responses and constricted visual fields, similar to our patient's electroretinographic findings of markedly reduced cone and 30-Hz flicker responses (fig. 2a) and paracentral visual field defects (fig. 3a). Also, 1 of the 3 previously reported patients [8] and our patient had retinal pigment epithelium atrophy along the vascular arcade. These findings raise the possibility that cone dysfunction may be caused in some patients with 1147delA mutation-positive Oguchi disease.

The homozygous 1147delA mutation has been also found in 3 Japanese patients with retinitis pigmentosa, in whom pigmentary retinal degeneration and constriction of visual fields were identified [16]. Furthermore, Yoshii et al. [10] described 3 patients with the homozygous 1147delA mutation in a Japanese family, 2 of whom were diagnosed with Oguchi disease and 1 of whom (III-1, in the source publication) was diagnosed with retinitis pigmentosa. The patient (III-1) had a loss of visual acuity and severely constricted visual fields [10]. Our patient's findings of funduscopy (fig. 1) and Goldmann visual fields (fig. 3b) can be differentiated from those of retinitis pigmentosa. Taken together, the 1147delA mutation is likely to be associated with variable clinical expression, ranging from Oguchi disease with/without retinal pigment epithelium atrophy along the vascular arcade to retinitis pigmentosa. Azam et al. [17] reported 8 Oguchi disease patients in a Pakistani family, who had been given a diagnosis of autosomal recessive retinitis pigmentosa before a *GRK1* mutation (Ser205stop) was identified. Thus, genetic testing is important to confirm the definitive diagnosis of Oguchi disease because retinitis pigmentosa caused by the homozygous 1147delA mutation is an extremely rare form of retinal degenerative disorder.

Relationships between macular function and morphology have not been studied in Oguchi disease patients with the 1147delA mutation. When comparing cone-mediated mf-ERG (fig. 2b) with anatomical features of the macula (fig. 1e, f), the preserved central responses (rings 1 and 2) can be explained by the well-preserved ISOS boundary lines in foveal and parafoveal areas, whereas the attenuated outer waveforms (rings 3–5) are most likely caused by ISOS boundary defects and thinning of the ONL outside the preserved ISOS boundary. Recently, the outer retinal architecture has been investigated using spectral domain OCT in a patient with Oguchi disease before and after prolonged dark adaptation, demonstrating that the undetectable ISOS boundary line at the paramacular area was clearly detected after 4 h of dark adaptation, although mutation analysis was not performed [18]. The thickness of the ONL did not change between before and after prolonged dark adaptation [18], which seems to be inconsistent with our OCT findings. In fact, we tried to perform OCT after a prolonged dark adaptation. Regrettably, cooperation of the patient was not obtained. The OCT findings in our patient are also seen in patients with progressive retinal degenerative diseases such as retinitis pigmentosa [19]. Our findings indicate that macular dysfunction secondary to attenuated cone function can occur in Oguchi disease patients with the 1147delA mutation.

In conclusion, the reduced/delayed mf-ERG responses and visual field defects in paracentral macula areas most likely correlate with ISOS boundary defects and thinning of the ONL. Further study is needed to investigate whether macular dysfunction is seen in other Oguchi disease patients with the 1147delA mutation in the *SAG* gene.

Acknowledgements

This work was supported by grants from the Ministry of Education, Culture, Sports, Science and Technology of Japan (Grant-in-Aid for Scientific Research) (T.H.), The Jikei University Research Fund (T.H.), and the Vehicle Racing Commemorative Foundation (T.H. and H.T.).

Disclosure Statement

The authors have no proprietary or financial interest in any aspect of this study.

References

1 Oguchi C: Ueber eine Abart von Hemeralopie (in Japanese). Nippon Ganka Gakkai Zasshi 1907;11:123–134.
2 Mizuo G: A novel finding associated with function of dark adaptation in Oguchi disease (in Japanese). Nippon Ganka Gakkai Zasshi 1913;17:1148–1150.
3 Miyake Y, Horiguchi M, Suzuki S, Kondo M, Tanikawa A. Electrophysiological findings in patients with Oguchi's disease. Jpn J Ophthalmol 1996;40:511–519.
4 Hashimoto H, Kishi S: Shortening of the rod outer segment in Oguchi disease. Graefes Arch Clin Exp Ophthalmol 2009;247:1561–1563.
5 Yamaki K, Tsuda M, Shinohara T: The sequence of human retinal S-antigen reveals similarities with alpha-transducin. FEBS Lett 1988;234:39–43.
6 Fuchs S, Nakazawa M, Maw M, Tamai M, Oguchi Y, Gal A: A homozygous 1-base pair deletion in the arrestin gene is a frequent cause of Oguchi disease in Japanese. Nat Genet 1995;10:360–362.
7 Yamamoto S, Sippel KC, Berson EL, Dryja TP: Defects in the rhodopsin kinase gene in the Oguchi form of stationary night blindness. Nat Genet 1997;15:175–178.
8 Nakazawa M, Wada Y, Fuchs S, Gal A, Tamai M: Oguchi disease: phenotypic characteristics of patients with the frequent 1147delA mutation in the arrestin gene. Retina 1997;17:17–22.
9 Nakamachi Y, Nakamura M, Fujii S, Yamamoto M, Okubo K: Oguchi disease with sectoral retinitis pigmentosa harboring adenine deletion at position 1147 in the arrestin gene. Am J Ophthalmol 1998;125:249–251.
10 Yoshii M, Murakami A, Akeo K, Nakamura A, Shimoyama M, Ikeda Y, Kikuchi Y, Okisaka S, Yanashima K, Oguchi Y: Visual function and gene analysis in a family with Oguchi's disease. Ophthalmic Res 1998,30:394–401.
11 Saga M, Mashima Y, Kudoh J, Oguchi Y, Shimizu N: Gene analysis and evaluation of the single founder effect in Japanese patients with Oguchi disease. Jpn J Ophthalmol 2004;48:350–352.
12 Yoshida S, Yamaji Y, Yoshida A, Ikeda Y, Yamamoto K, Ishibashi T: Rapid detection of *SAG* 926delA mutation using real-time polymerase chain reaction. Mol Vis 2006;12:1552–1557.
13 Takeuchi T, Hayashi T, Bedell M, Zhang K, Yamada H, Tsuneoka H: A novel haplotype with the R345W mutation in the *EFEMP1* gene associated with autosomal dominant drusen in a Japanese family. Invest Ophthalmol Vis Sci 2010;51:1643–1650.
14 Hayashi T, Gekka T, Takeuchi T, Goto-Omoto S, Kitahara K: A novel homozygous *GRK1* mutation (P391H) in 2 siblings with Oguchi disease with markedly reduced cone responses. Ophthalmology 2007;114:134–141.
15 Nakamura M, Yamamoto S, Okada M, Ito S, Tano Y, Miyake Y: Novel mutations in the arrestin gene and associated clinical features in Japanese patients with Oguchi's disease. Ophthalmology 2004;111:1410–1414.
16 Nakazawa M, Wada Y, Tamai M: Arrestin gene mutations in autosomal recessive retinitis pigmentosa. Arch Ophthalmol 1998;116:498–501.
17 Azam M, Collin RW, Khan MI, Shah ST, Qureshi N, Ajmal M, den Hollander AI, Qamar R, Cremers FP: A novel mutation in *GRK1* causes Oguchi disease in a consanguineous Pakistani family. Mol Vis 2009;15:1788–1793.
18 Yamada K, Motomura Y, Matsumoto CS, Shinoda K, Nakatsuka K: Optical coherence tomographic evaluation of the outer retinal architecture in Oguchi disease. Jpn J Ophthalmol 2009;53:449–451.
19 Sugita T, Kondo M, Piao CH, Ito Y, Terasaki H: Correlation between macular volume and focal macular electroretinogram in patients with retinitis pigmentosa. Invest Ophthalmol Vis Sci 2008;49:3551–3558.

Eur J Ophthalmol 2011; 21 (5): 657-660 DOI: 10.5301/EJO.2011.6337

CASE REPORT

Improvement in S-cone–mediated visual fields and rod function after correction of vitamin A deficiency

Takaaki Hayashi, Tamaki Gekka, Tadashi Nakano, Hiroshi Tsuneoka

Department of Ophthalmology, The Jikei University School of Medicine, Tokyo - Japan

PURPOSE. *To evaluate S-cone–mediated visual fields and full-field electroretinograms (ERGs) in a patient with vitamin A deficiency.*

METHODS. *A 65-year-old woman diagnosed with primary sclerosing cholangitis reported experiencing night blindness. The patient underwent comprehensive ophthalmic examination, including funduscopy, ERGs, Humphrey standard automated perimetry (SAP), and short-wavelength automated perimetry (SWAP). Serum vitamin A concentrations were measured.*

RESULTS. *The patient's best-corrected visual acuity was 1.2 in both eyes. The ERG results showed no rod b-waves, reduced combined rod-plus-cone responses (negative type), and normal cone and 30-Hz flicker responses. Serum vitamin A concentration was 18 IU/dL (normal range 97-316 IU/dL). The SAP mean deviation (MD) values were –1.09 dB (OD) and –0.97 dB (OS), whereas the SWAP MD values were –10.10 dB (OD) and –10.50 dB (OS). The rate of sensitivity decreased with increasing eccentricity in SWAP. Four months after starting oral administration of vitamin A, all ERG values were normalized, and SWAP MD values were greatly improved (OD –3.47 dB, OS –4.10 dB) compared with changes in SAP MD values (OD +0.67 dB, OS +0.41 dB). Rod dysfunction and impaired S-cone–mediated pathways were preferentially observed and found to be reversed after the treatment.*

CONCLUSIONS. *The findings in this patient suggest that rods and S cones are more susceptible to vitamin A deficiency than L and M cones. Vitamin A deficiency visual impairment may therefore be reversible with appropriate therapy.*

KEY WORDS. *Full-field electroretinography, Short wavelength automated perimetry, Vitamin A deficiency*

Accepted: January 3, 2011

INTRODUCTION

Vitamin A is crucial for ocular metabolism. In the retinoid visual cycle (1), the retinal pigment epithelium traps all-*trans* retinol from choroidal circulation, at which point all-*trans* retinol is metabolized and converted to the crucial chromophore 11-*cis* retinal. This retinal is then transported to the rod outer segments, where it binds to rod opsins to generate rhodopsin.

The vitamin A derivative 11-*cis* retinal is also crucial to maintaining the function of cone opsins, including short wavelength-sensitive (S), middle wavelength-sensitive (M), and long wavelength-sensitive (L) cone opsins. These photoreceptor cells are also known to be involved in visual dysfunction occurring due to vitamin A deficiency (VAD), with the first sign of VAD usually cited as night blindness, followed by other visual disturbances. In developed countries, VAD is generally due to poor intestinal absorption, liver dysfunction, or bile duct obstruction (2).

Primary sclerosing cholangitis (PSC) is a chronic, progressive cholestatic disease characterized by diffuse inflammation and fibrosis of both intrahepatic and extrahepatic bile ducts. However, the etiology and pathogenesis of PSC are not yet well-understood. Here, we describe a PSC patient with VAD in whom static visual fields and full-field electroretinograms (ERGs) were evaluated before and 4 months after vitamin A treatment.

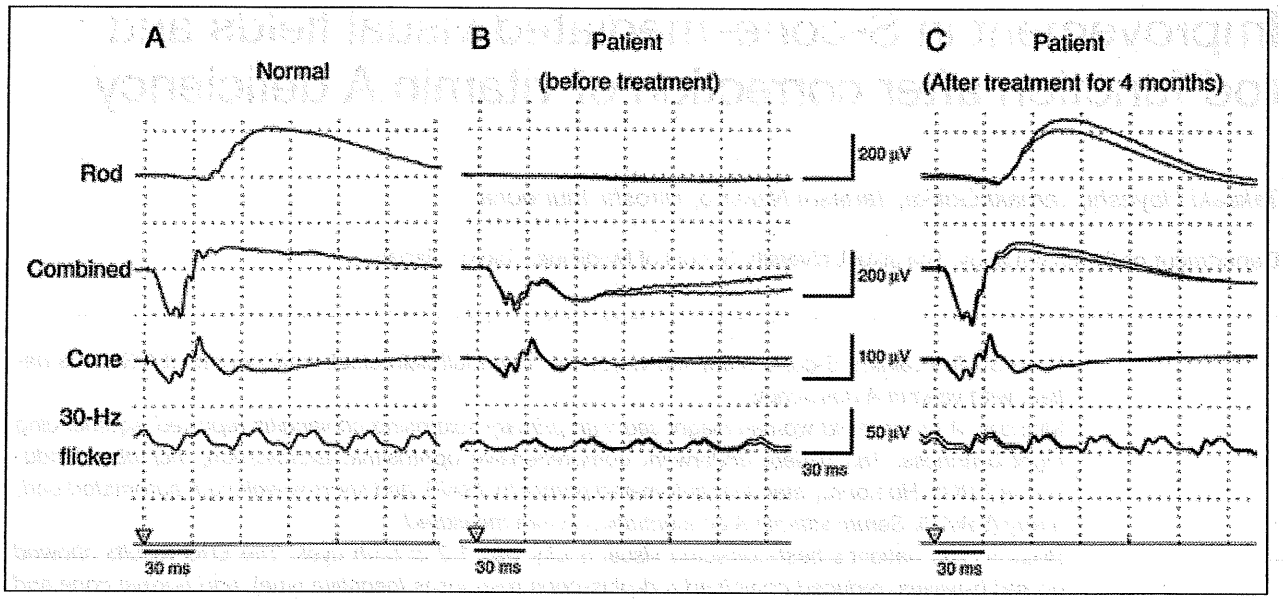

Fig. 1 - *Full-field electroretinograms (ERGs) from an age-matched normal subject with no retinal disease* **(A)** *and our vitamin A–deficient patient before* **(B)** *and 4 months after treatment* **(C)**. *Before treatment* **(B)**, *scotopic rod responses are undetectable, whereas photopic cone responses are well-preserved; however, the amplitudes of 30-Hz flicker ERGs are approximately half of normal* **(A)**. *Standard combined ERGs were negative-type with an additional a-wave amplitude reduction. Implicit times of all ERGs are nearly normal. After treatment* **(C)**, *all responses in rod, combined, cone, and 30-Hz flicker ERGs rebound to nearly normal levels.*

Case report

A 65-year-old Japanese woman was referred to our hospital following complaints of blurred vision and night blindness. She had been previously diagnosed with PSC, but had never had any ocular disease or received a blood transfusion. On initial evaluation at our hospital, the patient's best-corrected visual acuity was 1.2 in both eyes. No relative afferent pupillary defect was seen. Anterior segments and media were unremarkable except for the presence of mild senile cataracts in both eyes. Funduscopy showed no specific findings in either eye. Serum vitamin A concentration was markedly reduced at 18 IU/dL (normal range 97-316 IU/dL) (Tab. I). Electroretinogram were recorded according to the International Society for Clinical Electrophysiology of Vision protocol, as detailed previously (3). Scotopic rod responses were undetectable, whereas photopic cone responses were well-preserved; however, the amplitudes of 30-Hz flicker ERGs were approximately half of normal values (Fig. 1, A and B). Standard combined ERGs were negative-type with an additional a-wave amplitude reduction (Fig. 1B). Implicit times of rod, combined, cone, and 30-Hz flicker ERGs were nearly normal. Goldmann visual field testing was unremarkable.

We used the Humphrey Field Analyzer II (Carl Zeiss, Dublin, CA) to assess static visual fields, including central 30-2 Swedish interactive threshold algorithm (SITA), standard automated perimetry (SAP), and central 24-2 SITA short-wavelength automated perimetry (SWAP) programs. SWAP uses blue stimuli to stimulate S cones and a high-luminance yellow background to saturate L and M cones and rods (blue-on-yellow perimetry program). Mean deviation (MD), a global index that reflects overall depression in visual fields, was also evaluated. MD values for SITA-SAP were relatively well-preserved (–0.97 dB in OS, –1.09 dB in OD) (Fig. 2A). In contrast, SITA-SWAP results showed significant visual field loss, with MD values below –10 dB ($p<0.5\%$) in both eyes (Fig. 2C). The rate of sensitivity decreased with increasing eccentricity in SWAP (Fig. 2C). At this time, we confirmed that the impaired visual function was due to VAD secondary to PSC.

Treatment was initiated using oral administration of vitamin A (30,000 IU per day). At only 2 days after treatment, the serum vitamin A concentration had already increased to 95

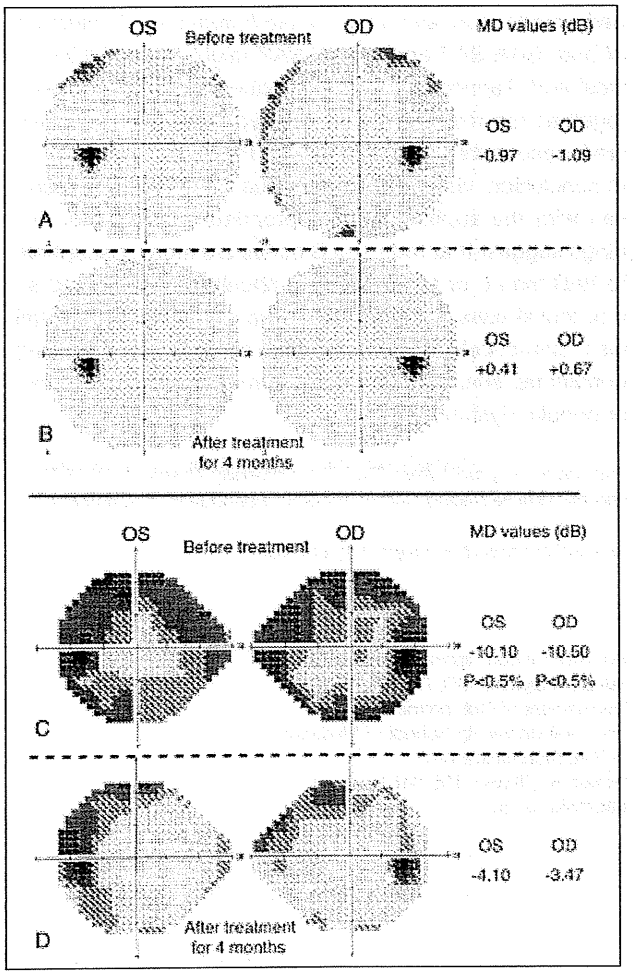

Fig. 2 - *Static visual fields using the Humphrey Field Analyzer II. Swedish interactive threshold algorithm (SITA)–standard automated perimetry (SAP) results before* **(A)** *and 4 months after treatment* **(B)**. *Swedish interactive threshold algorithm–standard automated perimetry results before* **(C)** *and 4 months after treatment* **(D)**. *See text for further details. Before treatment, MD values for SITA-SAP* **(A)** *are relatively well-preserved, whereas those for SITA-SWAP* **(C)** *are significantly low. After treatment, mean deviation (MD) values of SITA-SAP* **(B)** *remain unchanged or show subtle improvement, while SITA-SWAP* **(D)** *shows significant improvement in MD values.*

IU/dL (Tab. I), close to the normal range. The patient reported subjective improvements in night vision 4 to 8 weeks after treatment. Four months after the start of treatment, the ERG responses in rod, combined, cone, and 30-Hz flicker ERGs had rebounded to nearly normal levels (Fig. 1C). Mean deviation values of SITA-SAP remained unchanged or showed subtle improvement after treatment compared to before-treatment values (Fig. 2B), while SITA-SWAP showed significant improvement in MD values (–4.10 dB in OS and –3.47 in OD) (Fig. 2D). The patient continued to receive vitamin A treatment, and the concentration remained within the normal range for at least 7.5 months after treatment (Tab. I). The patient died of liver failure 16 months after initiation of vitamin A treatment.

DISCUSSION

With regard to ERG findings, before treatment, while the patient's rod responses were undetectable on ERG, the cone responses were relatively well-preserved (Fig. 1B), an observation consistent with the previous finding that rod dysfunction is typically observed earlier and is more extensive than cone dysfunction (2, 4). Although combined ERGs in most patients with VAD are subnormal, with reductions in both a-wave and b-wave amplitudes (4), the present patient showed negative ERG responses with reduced a-wave amplitudes, indicating not only the presence of photoreceptor abnormalities but also post-receptoral (or inner retinal transmission) dysfunction.

In their study, Newman et al (2) described 13 liver transplant candidates with VAD who were ophthalmologically asymptomatic, at least 5 of whom showed negative ERGs. The reason for the post-receptoral involvement remains unclear. Similar unexplained negative ERGs are also described in 34 cases of photoreceptor dystrophies reported by Koh et al (5), in keeping with previous reports on retinitis pigmentosa (RP), cone dystrophy, and cone-rod dystrophy (6). Additionally, Renner et al (7) described 47 patients with negative ERGs, 53% of whom had clinically suspected diagnoses (e.g., X-linked congenital retinoschisis, congenital stationary night blindness, and melanoma-associated reti-

TABLE I - SEQUENTIAL CHANGES IN SERUM VITAMIN A CONCENTRATION

Visit	Serum vitamin A concentration, IU/dL*
Before treatment	18
2 days after treatment	95
4 weeks after treatment	117
8 weeks after treatment	117
7.5 months after treatment	105

*Normal range: 97-316 IU/dL.